

Extensive electromechanical characterization of PZT thin films for MEMS applications by electrical and mechanical excitation signals

Klaus Prume · Paul Muralt · Florian Calame ·
Thorsten Schmitz-Kempen · Stephan Tiedke

Received: 19 March 2006 / Accepted: 21 August 2006 / Published online: 14 March 2007
© Springer Science + Business Media, LLC 2007

Abstract In this work we present a unique measurement method to estimate the effective transverse piezoelectric coefficient $e_{31,f}$ of piezoelectric thin films which is often used in micro electromechanical systems (MEMS). This method utilizes basically a 4-point bending setup specially adapted to be used with thin film samples. It allows the application of very homogeneous well defined mechanical stresses to the device. Stress and corresponding strain distribution are verified by Finite Element simulations. Measurements are shown to demonstrate the capability and repeatability of the setup on sol-gel processed PZT thin film samples. In conjunction with additional measurement results it is possible to fully determine the electromechanical characteristics.

Keywords Piezoelectric coefficients $d_{33,f}$ and $e_{31,f}$ · PZT thin film · 4-point bending · MEMS devices

1 Introduction

Piezoelectric thin films made e.g. of PZT (lead zirconate titanate) are widely used in MEMS devices [1]. Appropriate electrical and mechanical metrology is necessary for the characterization of these films and is essential for process specification and the design and

qualification of the devices. Pure electrical characterization methods like they have been developed for bulk ceramics and ferroelectric memory applications can be easily transferred to MEMS devices too. The well established and precise virtual ground measurement method allows the determination of polarization hysteresis and even capacitance and loss tangent [2].

This is different for the electromechanical responses of the device. The film and therefore device response on electrical or mechanical excitation is not a mere material characteristic of the piezoelectric thin film anymore but depends strongly on the underlying structure of substrate, interface and electrode layers and the processing parameters. For this reason effective longitudinal ($d_{33,f}$ see [3]) and transverse ($e_{31,f}$ see [4]) piezoelectric coefficients have been introduced to describe the piezoelectric behavior of thin films which are clamped on an underlying stiff substrate:

$$d_{33,f} = d_{33} - 2d_{31} \frac{s_{13}^E}{s_{11}^E + s_{12}^E} \quad (1)$$

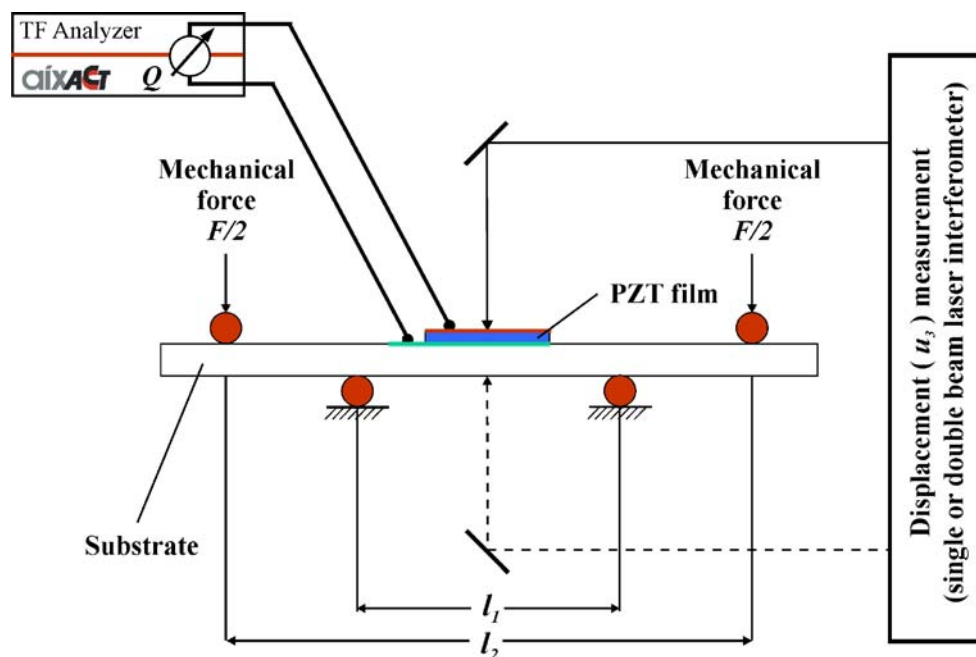
$$e_{31,f} = \frac{d_{31}}{s_{11}^E + s_{12}^E} = e_{31} + e_{33} \frac{s_{13}^E}{s_{11}^E + s_{12}^E} \quad (2)$$

where d_{ik} are the piezoelectric coefficients of an unclamped film and s_{ij}^E denote the mechanical compliances at constant electrical field E . The suffix f indicates that the effective coefficients are valid for boundary conditions of a film which is ideally clamped on a substrate. This means there is no strain in plane of the film respectively it is dictated by the strain of the substrate and it is free to move in the out of plane direction of the film.

K. Prume (✉) · T. Schmitz-Kempen · S. Tiedke
aixACCT Systems GmbH, Dennenwartstr. 25,
52068 Aachen, Germany
e-mail: prume@aixacct.com

P. Muralt · F. Calame
Laboratoire de Céramique, EPFL,
1015 Lausanne, Switzerland

Fig. 1 Measurement setup consisting of the aixACCT TF Analyzer, the 4-point bending sample holder, and a single respectively double beam laser interferometer



The most accurate method to determine the effective converse longitudinal piezoelectric coefficient $d_{33,f}$ of thin films in parallel to the poling direction is the double beam laser interferometry [5, 6]. In this method the sample strain is measured when an electrical field is applied to the sample. It extinguishes wafer bending influences due to the differential measurement with two laser beams to top and bottom of the wafer on the same spot.

Several methods have been developed to measure the effective direct transverse piezoelectric coefficient $e_{31,f}$ over the last years. Most of them imply the mechanically bending of a cantilever and measuring the current response [7–9]. In the described methods the challenge is to determine the exact mechanical strain the film is subjected to.

In this work we present a measurement setup which allows an easy and reliable way to determine electrical and electromechanical characteristics of piezoelectric thin film structures. Therefore, it allows the measurement of these characteristics which are important for MEMS devices on a single and simple producible test structure. The mechanical properties are mainly determined by the characteristics of the wafer type material as the thickness of the piezoelectric film is small in comparison to the underlying substrate structure.

2 Measurement setup

For precise measurements it is essential to have fixed and well defined boundary conditions of the

independent variables of the measurements. These independent variables are for example temperature, mechanical stress, and electric field. Isothermal temperature conditions can typically be assumed for the duration of a measurement. The electric field boundary conditions are well defined for typical capacitive structures with electrode areas much larger than the dielectric layer thickness. They are set by the attached electric circuitry. Whereas the mechanical stress boundary conditions are much more complicated to determine. Intrinsic stresses introduced by the different material layers, production processes, and environmental conditions all contribute to a mechanical prestress of the device. Part of this can be determined e.g. by wafer flexure methods. But in order to apply a well defined homogeneous stress distribution during the measurement special care must be taken. For this we propose a 4-point bending principle which is well established in mechanical materials testing to determine the flexural strength for ceramic bars [10]. A sample holder has been developed particularly adjusted to thin film structures (patent pending) which allows the application of well defined simultaneous electrical and mechanical excitation loads and the measurement of the corresponding sample response. The bending sample is placed in between four cylindrical supports like it is illustrated in Fig. 1.

The outer two supports with distance l_2 are both loaded with a mechanical force $F/2$ by a piezoelectric actuator. This induces a constant bending moment M on the test sample and therefore a homogeneous stress and strain distribution in the film between the inner

Table 1 Dimensions of the bending sample design.

Sample length	$l = 25 \text{ mm}$
Sample width	$b = 3 \text{ mm}$
Top electrode length	$l_{TE} = 10 \text{ mm}$
Top electrode width	$w_{TE} = 2 \text{ mm}$
Bottom electrode length	$l_{BE} = 4 \text{ mm}$
Wafer thickness	$h = 250 - 500 \mu\text{m}$

two supports of distance $l_1 = l_2/2$. The dimensions and design of the test samples are given in Table 1 and in Fig. 2.

Main control and measurement system is the TF Analyzer from aixACCT Systems. It runs the software to generate all required signals for electrical and mechanical excitation loads. Furthermore, the system simultaneously records all the sample responses. Different input channels are used to measure the induced charge, the voltage monitoring signal, and an electric signal from the interferometer which is proportional to the sample displacement.

3 Finite element simulations

Finite element simulations have been performed to prove the applicability of this 4-point bending principle on the thin film samples with their specific dimensions. A 3-dimensional bending sample model according to the sample geometry and layered film structure has been developed with the Finite Element program ANSYS™. Material properties have been taken from literature for the silicon wafer and the platinum electrodes. For the PZT film elastic coefficients of bulk material were used as the thin film values are hard to determine exactly. This model has been used to simulate a typical mechanical load case with an applied force of $F = 10 \text{ N}$ in 3-direction equally distributed on the two outer supports. Figure 3 displays the strain distribution in 1-direction of the film at the surface of the bending sample. Between the inner two supports

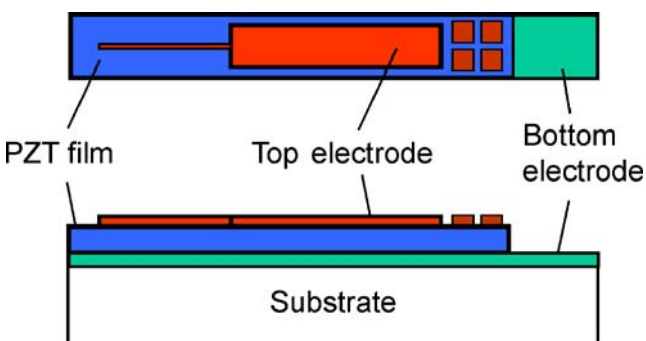


Fig. 2 Design of the bending samples

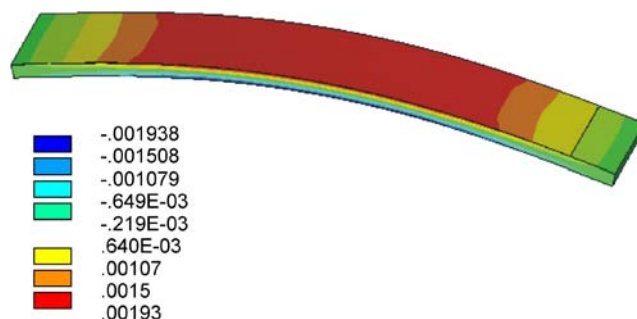


Fig. 3 Strain distribution in 1-direction of the sample under an applied force $F = 10 \text{ N}$

a homogeneous strain $S_1 = 0.00193$ can be observed which correlates to a maximum stress $T_1 = 269 \text{ MPa}$.

Under the assumption that the film thickness is very small in comparison to the substrate these results can be compared to an analytical calculation of strain and stress in a bending cantilever structure. The film will be exposed to the same constant strain as the strain S_1 of the surface layer of the bended silicon wafer. From mechanical textbooks the stress in the surface layer can be calculated to

$$T_1 = \frac{Mh}{2J_a} = \frac{3 Fl_1}{2 bh^2} \tag{3}$$

with the mechanical moment $M = \frac{Fl_1}{4}$ applied to the load span l_1 of the 4-point bending setup and the geometrical moment of inertia $J_a = \frac{bh^3}{12}$ of the silicon cantilever. b denotes in this case the width of the bending sample and h the thickness of the wafer.

The sample strain S_1 in the thin film is calculated by applying Hook's Law

$$S_1 = \frac{T_1}{E_{Si}} = \frac{3 Fl_1}{2 E_{Si} bh^2} \tag{4}$$

with the Young's modulus of the silicon substrate $E_{Si} = 130 \text{ GPa}$.

Stress and strain values obtained for an applied force of $F = 10 \text{ N}$ and geometrical sample parameter $l_2 = 20 \text{ mm}$, $l_1 = 10 \text{ mm}$, $b = 3 \text{ mm}$, $h = 450 \mu\text{m}$ compare good to the finite element findings:

$$\Rightarrow T_1 = \frac{3 Fl_1}{2 bh^2} = 247 \text{ MPa}$$

$$\Rightarrow S_1 = \frac{T_1}{E_{Si}} = 1.9 \cdot 10^{-3}$$

4 Measurement of the transverse piezoelectric coefficient

Now it is possible with this setup to apply an external alternating mechanical force to the sample and measure

Table 2 Processing differences for the measured samples.

Sample	Bottom electrode (machine)	Seed layer deposition
#1	BAS 450	Chemical solution deposition
#2	BAS 450	Reactive magnetron sputtering
#3	Nordiko	Reactive magnetron sputtering

the resulting bending with the laser system. The generated charge response on the electrodes is measured with the TF Analyzer. With the following assumptions and boundary conditions a direct correlation between $e_{31,f}$ and the measured charge and bending displacement can be derived [11]:

- The sample can freely expand and contract in 3-direction between the supports of the four point bending setup. Therefore no mechanical stress can occur in this direction.
- Induced charge Q is measured with a current amplifier using the virtual ground method so the electric field between the electrodes is zero.
- In plane strain in the thin film is equal to the strain at the surface of the bended substrate.

$$\Rightarrow e_{31,f} = \frac{Q}{A} \frac{(l_1/2)^2 + u_{3,cant}^2}{h u_{3,cant} (1 - \nu_{Si})} \quad (5)$$

therein A is the electrode area, ν_{Si} the Poisson coefficient of the silicon substrate, and $u_{3,cant}$ is the cantilever displacement due to sample bending measured in the middle of the sample. With $u_{3,cant} \ll l_1$ the equation can be further simplified to:

$$e_{31,f} \simeq \frac{Q l_1^2}{4 A h u_{3,cant} (1 - \nu_{Si})} \quad (6)$$

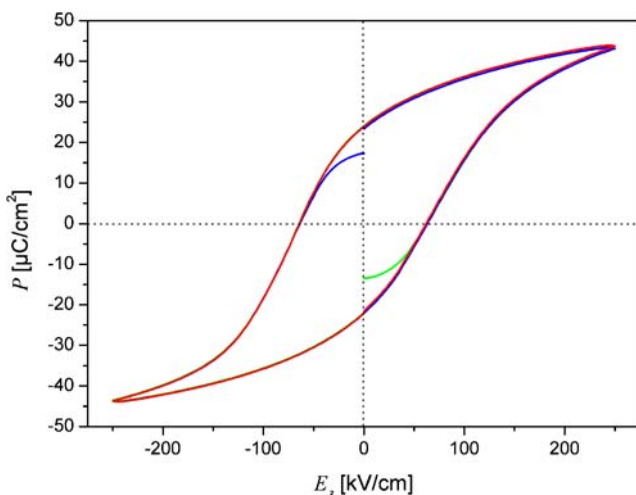


Fig. 4 Large signal electrical polarization of sample #3 at 1 Hz triangular excitation. The sample shows a relaxed remanent polarization $P_{rel+} = 17.3 \mu\text{C}/\text{cm}^2$ ($P_{rel-} = -13.5 \mu\text{C}/\text{cm}^2$) and a coercive field $E_{c+} = 62.0 \text{ kV}/\text{cm}$ ($E_{c-} = -64.1 \text{ kV}/\text{cm}$)

Small triangular force excitations result in linear displacement changes of the bending sample. The simultaneously measured charge plotted versus this displacement is for small signal conditions ideally a straight line. Its slope is proportional to the sought-after piezoelectric coefficient $e_{31,f}$. Results of these measurements are shown in the Measurement Result section.

5 Sample preparation

Test samples with PZT thin films were prepared with chemical solution deposition on $380 \mu\text{m}$ thick 4-inch wafers. A $1 \mu\text{m}$ thick wet oxide layer was grown in order to insulate the bottom electrode. For the latter, a 100 nm thick Pt(111) thin film was deposited on 15 nm thick TiO_2/Ti adhesion layer. A seeding layer of 100 oriented PbTiO_3 was deposited on the Pt bottom electrode in order to grow the PZT film in 100 crystalline orientation [12, 13]. The $1 \mu\text{m}$ thick $\text{Pb}(\text{Zr}_{53}\text{Ti}_{47})\text{O}_3$ film was deposited by the classical sol-gel route [14], which was optimized [15] with respect to lead excess and annealing procedure. A 100 nm thick Au/Cr top electrode was evaporated and patterned by lift-off. To access the bottom electrode, via holes were etched into the PZT film in a 40% HCl: HF solution at $60\text{--}65^\circ\text{C}$. Afterwards the wafer was diced into the desired test devices.

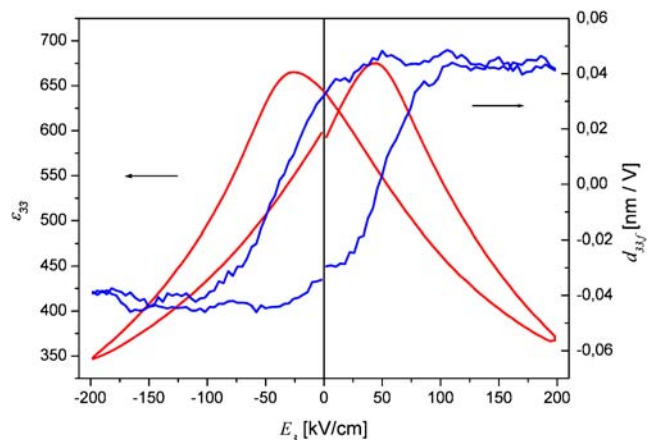


Fig. 5 Longitudinal piezoelectric response of sample #3 vs. applied DC bias field

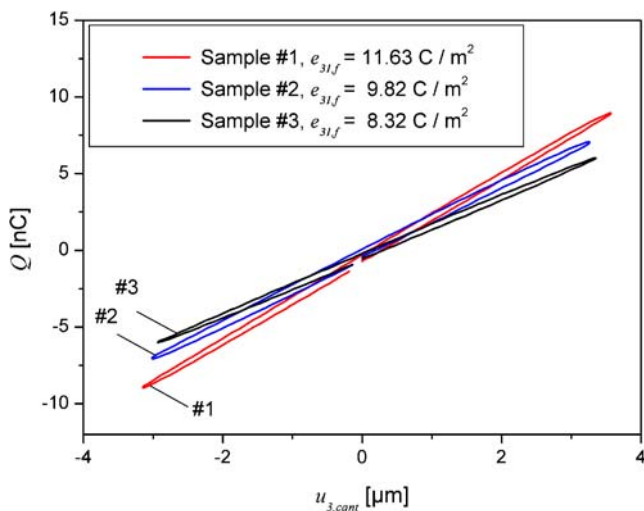


Fig. 6 Samples #1, #2, and #3 at 1 Hz and 10 V excitation of the piezo actuator

Three slightly different processing routes have been used for the samples which are investigated in this work. The differences between the samples are the deposition methods of the PbTiO_3 seed layer and are summarized in Table 2.

6 Measurement results

Starting with electrical measurement the electric polarization hysteresis is shown in Fig. 4 which gives good evidence on the quality of the deposited films. Remanent polarization and coercive field values are fundamental characteristics to compare different materials and compositions.

The small signal characterization of sample #3 in terms of dielectric ϵ_{33} and piezoelectric coefficient $d_{33,f}$ measurements is given in Fig. 5. It shows the dc bias dependent coefficients measured with double beam laser interferometry technique.

After these bipolar high field measurements the samples were poled for 10 min at 150 °C with a field of 200 kV/cm. In Fig. 6 measurements of the piezoelectric coefficient $e_{31,f}$ are shown on the three different samples mentioned before at 1 Hz excitation frequency and 10 V amplitude. More measurement results can be found in [11].

7 Conclusion

A comprehensive electrical and electromechanical characterization setup for piezoelectric thin film test

devices has been developed. This includes a 4-point bending sample holder which allows in combination with a laser interferometer the determination of the effective transverse piezoelectric coefficient $e_{31,f}$. Main advantage of this sample holder is the application of a precisely defined and homogeneous in plane strain to the film. The homogeneous strain distribution in the film was verified by finite element simulations. The same setup was used in conjunction with a double beam laser interferometer to measure the longitudinal piezoelectric response and typical electrical characteristics. Measurements to characterize the setup on PZT thin film test devices prepared by chemical solution deposition where shown.

Acknowledgements The authors wish to express their acknowledgments to the European Commission, who supported this work through the 6th Framework Project “MEMS-pie,” www.sintef.no/mems-pie. We thank the other industrial companies and research partners engaged in this project: Hök Instrument AB (Sweden), Noliac A/S (Denmark), Precision Acoustics Ltd. (UK), SINTEF (Norway), Sonitor Technologies AS (Norway), and University of Twente (The Netherlands).

References

1. P. Muralt, IEEE Trans. UFFC **47**, 903–915 (2000)
2. K. Prume, T. Schmitz, S. Tiedke, in *Polar Oxides—Properties, Characterization, and Imaging*, ed. by R. Waser, U. Böttger, S. Tiedke, (Wiley-VCH, 2004), ISBN 3-527-40532-1
3. K. Lefki, G.J.M. Dormans, J. Appl. Phys. **76**, 1764–1767 (1994)
4. P. Muralt, A. Kholkin, M. Kohli, T. Maeder, Sens. Actuators, A, Phys. **53**, 398–404 (1996)
5. A.L. Kholkin, C. Wüthrich, D.V. Taylor, N. Setter, Rev. Sci. Instrum. **67**, 1935–1941 (1996)
6. P. Gerber, A. Roelofs, O. Lohse, C. Kügeler, S. Tiedke, U. Böttger, R. Waser, Rev. Sci. Instrum. **74**, 2613–2615 (2003)
7. M.-A. Dubois, P. Muralt, Sens. Actuators **77**, 106–112 (1999)
8. J. Southin, S. Wilson, D. Schmitt, R. Whatmore, J. Phys. D: Appl. Phys. **34**, 1456–1460 (2001)
9. J.F. Shepard, P.J. Moses, S. Trolier-McKinstry, Sens. Actuators, A, Phys. **71**, 133–138 (1998)
10. ASTM, *C-1611-94: Standard test method for flexural strength of advanced ceramics at ambient temperature*. (American Society for Testing and Materials—West Conshohocken, PA, 1994)
11. K. Prume, P. Muralt, F. Calame, T. Schmitz-Kempen, S. Tiedke, IEEE Trans. UFFC **54**, 8–14 (2007)
12. T. Maeder, P. Muralt, M. Kohli, A. Kholkin, N. Setter, Br. Ceram. Proc. **54**, 206–218 (1995)
13. S. Hiboux, P. Muralt, N. Setter, Mater. Res. Soc. Symp. Proc. **595**, 499–504 (2000)
14. K.D. Budd, S.K. Dey, D.A. Payne, Br. Ceram. Proc. **36**, 107–121 (1985)
15. N. Ledermann, P. Muralt, J. Baborowski, S. Gentil, K. Mukati, M. Cantoni, A. Seifert, N. Setter, Sens. Actuators, A, Phys. **105**, 162–170 (2003)